Proceedings

of the

XXVI Congreso de Ecuaciones Diferenciales y Aplicaciones
XVI Congreso de Matemática Aplicada

Gijón (Asturias), Spain

June 14-18, 2021

SēMA
Sociedad Española
de Matemática Aplicada

Universidad de Oviedo

Editors:
Rafael Gallego, Mariano Mateos

Universidad de Oviedo
Servicio de Publicaciones de la Universidad de Oviedo
Campus de Humanidades. Edificio de Servicios. 33011 Oviedo (Asturias)
Tel. 985 10 95 03 Fax 985 10 95 07
http: www.uniovi.es/publicaciones
servipub@uniovi.es

ISBN: 978-84-18482-21-2

Foreword

It is with great pleasure that we present the Proceedings of the 26th Congress of Differential Equations and Applications / 16th Congress of Applied Mathematics (XXVI CEDYA / XVI CMA), the biennial congress of the Spanish Society of Applied Mathematics S$\vec{e}$MA, which is held in Gijón, Spain from June 14 to June 18, 2021.

In this volume we gather the short papers sent by some of the almost three hundred and twenty communications presented in the conference. Abstracts of all those communications can be found in the abstract book of the congress. Moreover, full papers by invited lecturers will shortly appear in a special issue of the S$\vec{e}$MA Journal.

The first CEDYA was celebrated in 1978 in Madrid, and the first joint CEDYA / CMA took place in Málaga in 1989. Our congress focuses on different fields of applied mathematics: Dynamical Systems and Ordinary Differential Equations, Partial Differential Equations, Numerical Analysis and Simulation, Numerical Linear Algebra, Optimal Control and Inverse Problems and Applications of Mathematics to Industry, Social Sciences, and Biology. Communications in other related topics such as Scientific Computation, Approximation Theory, Discrete Mathematics and Mathematical Education are also common.

For the last few editions, the congress has been structured in mini-symposia. In Gijón, we will have eighteen minis-symposia, proposed by different researchers and groups, and also five thematic sessions organized by the local organizing committee to distribute the individual contributions. We will also have a poster session and ten invited lectures. Among all the mini-symposia, we want to highlight the one dedicated to the memory of our colleague Francisco Javier "Pancho" Sayas, which gathers two plenary lectures, thirty-six talks, and more than forty invited people that have expressed their wish to pay tribute to his figure and work.

This edition has been deeply marked by the COVID-19 pandemic. First scheduled for June 2020, we had to postpone it one year, and move to a hybrid format. Roughly half of the participants attended the conference online, while the other half came to Gijón. Taking a normal conference and moving to a hybrid format in one year has meant a lot of efforts from all the parties involved. Not only did we, as organizing committee, see how much of the work already done had to be undone and redone in a different way, but also the administration staff, the scientific committee, the mini-symposia organizers, and many of the contributors had to work overtime for the change.

Just to name a few of the problems that all of us faced: some of the already accepted mini-symposia and contributed talks had to be withdrawn for different reasons (mainly because of the lack of flexibility of the funding agencies); it became quite clear since the very first moment that, no matter how well things evolved, it would be nearly impossible for most international participants to come to Gijón; reservations with the hotels and contracts with the suppliers had to be cancelled; and there was a lot of uncertainty, and even anxiety could be said, until we were able to confirm that the face-to-face part of the congress could take place as planned.

On the other hand, in the new open call for scientific proposals, we had a nice surprise: many people that would have not been able to participate in the original congress were sending new ideas for mini-symposia, individual contributions and posters. This meant that the total number of communications was about twenty percent greater than the original one, with most of the new contributions sent by students.

There were almost one hundred and twenty students registered for this CEDYA / CMA. The hybrid format allows students to participate at very low expense for their funding agencies, and this gives them the opportunity to attend different conferences and get more merits. But this, which can be seen as an advantage, makes it harder for them to obtain a full conference experience. Alfréd Rényi said: "a mathematician is a device for turning coffee into theorems". Experience has taught us that a congress is the best place for a mathematician to have a lot of coffee. And coffee cannot be served online.

In Gijón, June 4, 2021

The Local Organizing Committee from the Universidad de Oviedo

Scientific Committee

- Juan Luis Vázquez, Universidad Autónoma de Madrid
- María Paz Calvo, Universidad de Valladolid
- Laura Grigori, INRIA Paris
- José Antonio Langa, Universidad de Sevilla
- Mikel Lezaun, Euskal Herriko Unibersitatea
- Peter Monk, University of Delaware
- Ira Neitzel, Universität Bonn
- JoséÁngel Rodríguez, Universidad de Oviedo
- Fernando de Terán, Universidad Carlos III de Madrid

Sponsors

- Sociedad Española de Matemática Aplicada
- Departamento de Matemáticas de la Universidad de Oviedo
- Escuela Politécnica de Ingeniería de Gijón
- Gijón Convention Bureau
- Ayuntamiento de Gijón

Local Organizing Committee from the Universidad de Oviedo

- Pedro Alonso Velázquez
- Rafael Gallego
- Mariano Mateos
- Omar Menéndez
- Virginia Selgas
- Marisa Serrano
- Jesús Suárez Pérez del Río

Contents

On numerical approximations to diffuse-interface tumor growth models
Acosta-Soba D., Guillén-González F. and Rodríguez-Galván J.R. **8**

An optimized sixth-order explicit RKN method to solve oscillating systems
Ahmed Demba M., Ramos H., Kumam P. and Watthayu W. **15**

The propagation of smallness property and its utility in controllability problems
Apraiz J. **23**

Theoretical and numerical results for some inverse problems for PDEs
Apraiz J., Doubova A., Fernández-Cara E. and Yamamoto M. **31**

Pricing TARN options with a stochastic local volatility model
Arregui I. and Ráfales J. **39**

XVA for American options with two stochastic factors: modelling, mathematical analysis and numerical methods
Arregui I., Salvador B., Ševčovič D. and Vázquez C. **44**

A numerical method to solve Maxwell's equations in 3D singular geometry
Assous F. and Raichik I. **51**

Analysis of a SEIRS metapopulation model with fast migration
Atienza P. and Sanz-Lorenzo L. **58**

Goal-oriented adaptive finite element methods with optimal computational complexity
Becker R., Gantner G., Innerberger M. and Praetorius D. **65**

On volume constraint problems related to the fractional Laplacian
Bellido J.C. and Ortega A. **73**

A semi-implicit Lagrange-projection-type finite volume scheme exactly well-balanced for 1D shallow-water system
Caballero-Cárdenas C., Castro M.J., Morales de Luna T. and Muñoz-Ruiz M.L. **82**

SEIRD model with nonlocal diffusion
Calvo Pereira A.N. **90**

Two-sided methods for the nonlinear eigenvalue problem
Campos C. and Roman J.E. **97**

Fractionary iterative methods for solving nonlinear problems
Candelario G., Cordero A., Torregrosa J.R. and Vassileva M.P. **105**

Well posedness and numerical solution of kinetic models for angiogenesis
Carpio A., Cebrián E. and Duro G. **109**

Variable time-step modal methods to integrate the time-dependent neutron diffusion equation
Carreño A., Vidal-Ferràndiz A., Ginestar D. and Verdú G. **114**

Homoclinic bifurcations in the unfolding of the nilpotent singularity of codimension 4 in R^4
Casas P.S., Drubi F. and Ibánez S. **122**

Different approximations of the parameter for low-order iterative methods with memory
Chicharro F.I., Garrido N., Sarría I. and Orcos L. **130**

Designing new derivative-free memory methods to solve nonlinear scalar problems
Cordero A., Garrido N., Torregrosa J.R. and Triguero P. **135**

Iterative processes with arbitrary order of convergence for approximating generalized inverses
Cordero A., Soto-Quirós P. and Torregrosa J.R. **141**

FCF formulation of Einstein equations: local uniqueness and numerical accuracy and stability
Cordero-Carrión I., Santos-Pérez S. and Cerdá-Durán P. **148**

New Galilean spacetimes to model an expanding universe
De la Fuente D. **155**

Numerical approximation of dispersive shallow flows on spherical coordinates
Escalante C. and Castro M.J. **160**

New contributions to the control of PDEs and their applications
Fernández-Cara E. **167**

Saddle-node bifurcation of canard limit cycles in piecewise linear systems
Fernández-García S., Carmona V. and Teruel A.E. **172**

On the amplitudes of spherical harmonics of gravitational potencial and generalised products of inertia
Floría L. **177**

Turing instability analysis of a singular cross-diffusion problem
Galiano G. and González-Tabernero V. **184**

Weakly nonlinear analysis of a system with nonlocal diffusion
Galiano G. and Velasco J. **192**

What is the humanitarian aid required after tsunami?
González-Vida J.M., Ortega S., Macías J., Castro M.J., Michelini A. and Azzarone A. **197**

On Keller-Segel systems with fractional diffusion
Granero-Belinchón R. **201**

An arbitrary high order ADER Discontinous Galerking (DG) numerical scheme for the multilayer shallow water model with variable density
Guerrero Fernández E., Castro Díaz M.J., Dumbser M. and Morales de Luna T. **208**

Picard-type iterations for solving Fredholm integral equations
Gutiérrez J.M. and Hernández-Verón M.A. **216**

High-order well-balanced methods for systems of balance laws based on collocation RK ODE solvers
Gómez-Bueno I., Castro M.J., Parés C. and Russo G. **220**

An algorithm to create conservative Galerkin projection between meshes
Gómez-Molina P., Sanz-Lorenzo L. and Carpio J. **228**

On iterative schemes for matrix equations
Hernández-Verón M.A. and Romero N. **236**

A predictor-corrector iterative scheme for improving the accessibility of the Steffensen-type methods
Hernández-Verón M.A., Magreñán A.A., Martínez E. and Sukhjit S. **242**

CONTENTS

Recent developments in modeling free-surface flows with vertically-resolved velocity profiles using moments
Koellermeier J. **247**

Stability of a one degree of freedom Hamiltonian system in a case of zero quadratic and cubic terms
Lanchares V. and Bardin B. **253**

Minimal complexity of subharmonics in a class of planar periodic predator-prey models
López-Gómez J., Muñoz-Hernández E. and Zanolin F. **258**

On a non-linear system of PDEs with application to tumor identification
Maestre F. and Pedregal P. **265**

Fractional evolution equations in dicrete sequences spaces
Miana P.J. **271**

KPZ equation approximated by a nonlocal equation
Molino A. **277**

Symmetry analysis and conservation laws of a family of non-linear viscoelastic wave equations
Márquez A. and Bruzón M. **284**

Flux-corrected methods for chemotaxis equations
Navarro Izquierdo A.M., Redondo Neble M.V. and Rodríguez Galván J.R. **289**

Ejection-collision orbits in two degrees of freedom problems
Ollé M., Álvarez-Ramírez M., Barrabés E. and Medina M. **295**

Teaching experience in the Differential Equations Semi-Virtual Method course of the Tecnológico de Costa Rica
Oviedo N.G. **300**

Nonlinear analysis in lorentzian geometry: the maximal hypersurface equation in a generalized Robertson-Walker spacetime
Pelegrín J.A.S. **307**

Well-balanced algorithms for relativistic fluids on a Schwarzschild background
Pimentel-García E., Parés C. and LeFloch P.G. **313**

Asymptotic analysis of the behavior of a viscous fluid between two very close mobile surfaces
Rodríguez J.M. and Taboada-Vázquez R. **321**

Convergence rates for Galerkin approximation for magnetohydrodynamic type equations
Rodríguez-Bellido M.A., Rojas-Medar M.A. and Sepúlveda-Cerda A. **325**

Asymptotic aspects of the logistic equation under diffusion
Sabina de Lis J.C. and Segura de León S. **332**

Analysis of turbulence models for flow simulation in the aorta
Santos S., Rojas J.M., Romero P., Lozano M., Conejero J.A. and García-Fernández I. **339**

Overdetermined elliptic problems in onduloid-type domains with general nonlinearities
Wu J. **344**

XXVI Congreso de Ecuaciones Diferenciales y Aplicaciones
XVI Congreso de Matemática Aplicada
Gijón, 14-18 junio 2021
(pp. 208–215)

An arbitrary high order ADER Discontinous Galerking (DG) numerical scheme for the multilayer shallow water model with variable density

E. Guerrero Fernández [1], M.J. Castro Díaz[1], M. Dumbser[2], T. Morales de Luna[3]

1. *Departamento de Análisis Matemático, Facultad de Ciencias, Universidad de Málaga, Campus de Teatinos S/N, 29081 Málaga, Spain.*
2. *Department of Civil, Environmental and Mechanical Engineering, Via Mesiano, 77 - 38123 Trento, Italy.*
3. *Departamento de Matemáticas, Universidad de Córdoba, Campus de Rabanales, 14071 Córdoba, Spain.*

Abstract

In this work, an arbitrary high order numerical discretization for a density dependent multilayer shallow-water model is presented. The model can be written as a system of hyperbolic PDE equations and it is especially suited for simulations of density driven gravity currents within the shallow-water framework. The proposed discretization is composed by an unlimited high order accurate (ADER) Discontinuous Galerkin (DG) method, which is then limited *a posteriori* with the MOOD paradigm, resulting in great resolution capabilities in smooth regions alongside a robust and accurate respond for strong gradients or discontinuities. A numerical strategy to preserve non-trivial stationary solutions is also discussed. Some numerical results are shown including density driven currents where laboratory data is available.

1. Introduction

A wildly used model for the simulation of geophysical flows is shallow-water (or Saint-Venant) model. In shallow-water flows, the vertical component of the velocity is neglected and the horizontal component is assumed to be constant along the vertical direction. In this way, the dimension of the problem is reduced by one, allowing to improve dramatically the computational times for large scale simulations. This approach has been successfully used in many practical applications (see [10, 18, 19]). However, the horizontally constant velocity hypothesis can seriously limit the amount of information that the model is able to provide and that may be relevant for the problem. To address this issue, multilayer shallow-water models are developed, where the vertical direction is subsequently divided in computational layers and the shallow-water hypotheses are performed in each layer individually (see [4, 5]). This allows, for instance, to recover a detailed vertical profile of the velocity and the cost of a slightly higher computational times. Of course, some mechanism for the interaction between layers must be considered. For instance, [7, 17] assume immiscible layers meanwhile for multilayer shallow-water systems considered in [3, 15], a continuous mass and momentum exchange between the layers is considered. The incorporation of the mass and momentum transfer between layers is performed via non-conservative terms. The multilayer shallow-water model considered in this work includes density effects throughout density dependent pressure terms. A full description of the derivation of the model can be found at [16] and [2].

The Discontinuous Galerkin (DG) method itself dates back to the early work by Reed and Hill in [21]. This methods allows to easily reach high order in space. In more recent work, it is combined with an arbitrary high order derivatives (ADER) procedure, which allows to reach arbitrary high order in time (see [12]). The ADER approach is based on the approximated solution of Riemann problems by means of a fixed point algorithm in each element locally. This combination leads naturally to high order, single step and fully discrete numerical schemes. However, this approach is unlimited, in the sense that there is no mechanism to prevent the apparition of spurious oscillations near strong gradients or discontinuities. As a limiting technique, we use a multi-dimensional optimal order detection (MOOD) (see [13]), which is *a posteriori* approach to the problem of limiting. The unlimited solution of the ADER-DG scheme is tested to study its admissibility in terms of spurious oscillations but also other physical criteria like positivity. If the solution is found inadequate, then the MOOD technique will switch to a robust second order accurate finite volume method in order to compute the limited solution.

Another issue of paramount importance for the long time numerical stability of the numerical scheme are the ability of the scheme to preserve stationary solutions ([6, 9]). Indeed, many practical applications often consist on a perturbation of an *equilibria* state, and thus exactly preserving this state is of great importance. Here, we propose a procedure to exactly preserve non-trivial stationary solutions in the ADER-DG framework.

Due to space restrictions, these techniques will be presented in a non-exhaustive manner. However, the interested reader has references available throughout the text.

2. Model description

Here, we briefly present the density dependent multilayer shallow-water model considered in this work. A full description and derivation of the model can be found at [16]. The full system of equations for the model in one dimension is,

$$\begin{cases} \partial_t h + \partial_x \left(h \sum_{\beta=1}^{M} u_\beta \right) = 0, \\ \partial_t (h\theta_\alpha) + \partial_x (h\theta_\alpha u_\alpha) = \dfrac{1}{l_\alpha} \left(\theta_{\alpha+\frac{1}{2}} G_{\alpha+\frac{1}{2}} - \theta_{\alpha-\frac{1}{2}} G_{\alpha-\frac{1}{2}} \right), \\ \partial_t (h\theta_\alpha u_\alpha) + \partial_x (h\theta_\alpha u_\alpha^2) + g h \theta_\alpha \partial_x \eta + \dfrac{g\, l_\alpha}{2} \left(h\partial_x (h\theta_\alpha) - h\theta_\alpha \partial_x h \right) \\ + g \sum_{\beta=\alpha+1}^{M} l_\beta \left(h\partial_x (h\theta_\beta) - h\theta_\alpha \partial_x h \right) = \dfrac{1}{l_\alpha} \left(u_{\alpha+\frac{1}{2}} \theta_{\alpha+\frac{1}{2}} G_{\alpha+\frac{1}{2}} - u_{\alpha-\frac{1}{2}} \theta_{\alpha-\frac{1}{2}} G_{\alpha-\frac{1}{2}} \right), \end{cases} \tag{2.1}$$

where h is the total height of the water column, $\eta = h + z_b$ is the free surface, and z_b is the bathymetry function. Additionally, u_α refers to the horizontal velocity while θ_α is the relative density of the fluid in the α-layer. Finally, $G_{\alpha\pm\frac{1}{2}}$ $\alpha = 1, \ldots, M$, are the mass transference terms between layers.

System (2.1) is obtained under the closure hypothesis that the layer thickness is proportional to the total height, $h_\alpha = l_\alpha h$, with $l_\alpha \in [0, 1]$, $\alpha = 1, \ldots, M$ such that $\sum_{\alpha=1}^{M} l_\alpha = 1$. Under this assumption, we are able to give an expression for the mass transference terms,

$$G_{\alpha+\frac{1}{2}} = \sum_{\beta=1}^{\alpha} l_\beta \left(\partial_t h + \partial_x (h u_\beta) \right) = \sum_{\beta=1}^{\alpha} l_\beta \left(\partial_x (h u_\beta) - \partial_x \left(\sum_{\gamma=1}^{M} l_\gamma h u_\gamma \right) \right). \tag{2.2}$$

We assume no mass transference at the bottom and free surface, $G_{1/2} = G_{M+1/2} = 0$, and $\theta_{\alpha+1/2}$ and $u_{\alpha+1/2}$ are some approximations of u and θ at the layers interfaces, for example a simple arithmetic mean. Note that the full system (2.1) reduces to the standard shallow water equations for the particular case $M = 1$ and $\theta = 1$.

The full PDE system (2.1) has an infinity number of stationary solutions. Indeed, the standard shallow-water stationary solutions with constant free surface η are also solution of the system (2.1) if a homogeneous density profile is considered,

$$\theta_\alpha = \text{cte}, \quad u_\alpha = 0, \quad \text{for } \alpha = 1, \ldots, M, \quad \eta = \text{cte}.$$

However, system (2.1) also admits lake-at-rest stationary solutions corresponding to non-trivial density profiles. Stationary solutions with $u_\alpha = 0$, $\alpha = 1, \ldots, M$ for the system (2.1) correspond to the solutions of the following ODE system,

$$P_\alpha := g h \theta_\alpha \partial_x \eta + \frac{g l_\alpha}{2} \left(h\partial_x (h\theta_\alpha) - h\theta_\alpha \partial_x h \right) + g \sum_{\beta=\alpha+1}^{M} l_\beta \left(h\partial_x (h\theta_\beta) - h\theta_\alpha \partial_x h \right) = 0. \tag{2.3}$$

Once the free surface is fixed, this equation can be solved iteratively by solving first the upper layer and sequentially going downwards throughout the lower layers. In particular we are interested in those with a constant free surface and a vertically stratified density profile, that is,

$$\eta(x) = h(x) + z_b(x) = \text{cte}, \qquad \theta(z) = \theta_{surface} + \gamma(\eta - z). \tag{2.4}$$

Unfortunately, due to the numerical discretization performed on the full system of PDE equations (2.1), this profile is not a stationary solution of (2.3) and cannot be directly preserved unless the bathymetry is the constant function. However, system (2.3) can be solved recursively, which results into a stratified density profile that could be seen as an approximation of (2.4) associated to the multilayer approach. In particular, those solutions are given by the following expression,

$$\begin{gathered} u_\alpha = 0, \ \eta(x) = z_b(x) + h(x) = \text{cte}, \\ \theta_M(x) = \bar{\theta}_M \geq 1, \\ \theta_\alpha(x) = \bar{\theta}_\alpha \, h^{2(M-\alpha)}(x) + \sum_{\beta=\alpha+1}^{M} S_{2(M-\beta)}(M - \alpha + 1) \bar{\theta}_\beta \, h^{2(M-\beta)}(x), \end{gathered} \tag{2.5}$$

with

$$\begin{aligned} S_\beta(\alpha) &= (\beta+1)\cdot A_{\frac{\beta+2}{2}+1}(\alpha), \\ A_p(k) &= \begin{cases} 1 & \text{if } p \geq k, \\ (p-1)\prod_{\gamma=2}^{k-p}(1+(p-2)C_{\gamma-1}) & \text{if } p < k, \end{cases} \\ C_\gamma &= C_{\gamma-1} - \frac{1}{Q_\gamma}, \\ Q_\gamma &= Q_{\gamma-1} + \gamma + 1, \\ C_0 &= Q_0 = 1, \end{aligned}$$

where $\bar{\theta}_\alpha$ is a free choice constant fixed by the initial conditions, that determines the vertical profile of the density.

For more details relative to this model, we refer the reader to [16].

3. Numerical discretization

In this section we provide brief description of the numerical scheme used on (2.1). If the interested reader wants to know more we refer them to [13, 14].

System (2.1) may be written as follows,

$$\partial_t \boldsymbol{w} + \partial_x \boldsymbol{F}_C(\boldsymbol{w}) + \boldsymbol{P}(\boldsymbol{w}, \partial_x \boldsymbol{w}, \partial_x \eta) - \boldsymbol{T}(\boldsymbol{w}, \partial_x \boldsymbol{w}) = \boldsymbol{0}, \tag{3.1}$$

where $\boldsymbol{w}$ is the vector of the conserved variables,

$$\boldsymbol{w} = (h \,|\, h\theta_\alpha \,|\, h\theta_\alpha u_\alpha)^T \in \mathbb{R}^{2M+1}, \tag{3.2}$$

the physical convective flux $F_C(\boldsymbol{w})$ is given by,

$$F_C(\boldsymbol{w}) = \left(hu_\alpha \,|\, h\theta_\alpha u_\alpha \,|\, h\theta_\alpha u_\alpha^2\right)^T \in \mathbb{R}^{2M+1}, \tag{3.3}$$

and $\boldsymbol{P}(\boldsymbol{w}, \partial_x \boldsymbol{w}, \partial_x \eta)$ corresponds to the pressure term, which depends on the relative density θ_α and the free surface η, and has the following form,

$$\boldsymbol{P}(\boldsymbol{w}, \partial_x \boldsymbol{w}, \partial_x \eta) = (\boldsymbol{0} \,|\, \boldsymbol{0} \,|\, P_\alpha) \in \mathbb{R}^{2M+1}, \tag{3.4}$$

where

$$P_\alpha = gh\theta_\alpha \partial_x \eta + \frac{g\, l_\alpha}{2}(h\partial_x(h\theta_\alpha) - h\theta_\alpha \partial_x h) + g\sum_{\beta=\alpha+1}^{M} l_\beta (h\partial_x(h\theta_\beta) - h\theta_\alpha \partial_x h). \tag{3.5}$$

Finally, the term $\boldsymbol{T}(\boldsymbol{w}, \partial_x \boldsymbol{w})$ corresponds to the mass, density, and momentum exchange between layers:

$$\boldsymbol{T}(\boldsymbol{w}, \partial_x \boldsymbol{w}) = \left(0 \,\middle|\, \frac{1}{l_\alpha}\left(\theta_{\alpha+\frac{1}{2}} G_{\alpha+\frac{1}{2}} - \theta_{\alpha-\frac{1}{2}} G_{\alpha-\frac{1}{2}}\right) \,\middle|\, \frac{1}{l_\alpha}\left(u_{\alpha+\frac{1}{2}}\theta_{\alpha+\frac{1}{2}} G_{\alpha+\frac{1}{2}} - u_{\alpha-\frac{1}{2}}\theta_{\alpha-\frac{1}{2}} G_{\alpha-\frac{1}{2}}\right)\right)^T \in \mathbb{R}^{2M+1}. \tag{3.6}$$

The system of equations (3.1) is solved by applying the family of pure Discontinuous Galerkin methods $\mathbb{P}_N\mathbb{P}_N$. The numerical scheme is formulated as a predictor-corrector method: in the first step, a predictor solution, which consist on a high order approximation of the solution at the following time step, is computed by means of a local Cauchy problem, without interaction with the neighbours states. In the next step, the corrector will make use of these predictor solution to compute a high order in space and time approximation of the solution of system (2.1) at the next time step.

The usual one dimensional considerations relative to the domain discretizations into non-overlaping conforming set of elements are considered. The computation domain Ω is discretized into $T_i = [x_{i-\frac{1}{2}}, x_{i+\frac{1}{2}}]$, $i = 1, \ldots, N_s$ elements, where N_s is the total number of cells with a constant length $\Delta x = x_{i+\frac{1}{2}} - x_{i-\frac{1}{2}}$.

We will make use of the following notation: for any variable f defined on a volume T_i, we will denote by $f_{i\pm\frac{1}{2}}$ the values at the interface, depending on whether it is the right or left side of the cell. However, when the values correspond to projected states into the interface, it will be generally denoted with the super index $f^\pm$, depending on whether they correspond to the left or to the right side of the intercell.

In the following, the discrete solution of the PDE system (3.1) at time t^n is denoted by $\boldsymbol{w}_h(x, t^n)$ and is defined in terms of piecewise polynomials of degree N on the spatial direction. We shall denote by $\mathcal{U}_h$ the space of piecewise polynomials up to degree N so that $\boldsymbol{w}_h(\cdot, t^n) \in \mathcal{U}_h$. In this work, a nodal basis defined by the Lagrange

interpolation polynomials over the $(N+1)$ Gauss-Legendre quadrature nodes on the element T_i is adopted. As usual in the discontinuous Galerkin (DG) approach, the discrete solution $\boldsymbol{w}_h$ may be discontinuous across the intercells, as in finite volume methods. At each cell T_i, the discrete solution is written in terms of the nodal spatial basis functions $\Phi_l(x)$ and some unknown degrees of freedom $\hat{\boldsymbol{w}}_{i,l}^n$,

$$\boldsymbol{w}_h(x,t^n) = \sum_l \hat{\boldsymbol{w}}_{i,l}^n \Phi_l(x) := \hat{\boldsymbol{w}}_{i,l}^n \Phi_l(x), \qquad \text{for } x \in T_i, \tag{3.7}$$

where the Einstein summation convention over two repeated indices has been considered. The spatial basis functions are defined on the reference interval $[0,1]$.

The ADER-DG method results from multiplying the governing PDE system (3.1) with a test function $\Phi_k \in \mathcal{U}_h$ and integrate over the space-time control volume $T_i \times [t^n, t^{n+1}]$. This results in the expression,

$$\int_{t^n}^{t^{n+1}} \int_{T_i} \Phi_k \partial_t \boldsymbol{w}\, dxdt \;+\; \int_{t^n}^{t^{n+1}} \int_{T_i} \Phi_k \left(\partial_x \boldsymbol{F}_C(\boldsymbol{w})\, dxdt + \boldsymbol{P}(\boldsymbol{w}, \partial_x \boldsymbol{w}, \partial_x \eta) - \boldsymbol{T}(\boldsymbol{w}, \partial_x \boldsymbol{w})\right) dxdt \;=\; \boldsymbol{0}. \tag{3.8}$$

The discrete solution $\boldsymbol{w}_h(x,t^n)$ is allowed to jump across element interfaces, which means that the resulting jump terms have to be properly taken into account. In our scheme this is achieved via numerical flux functions in the form of approximate Riemann solvers that follows the path-conservative approach that was developed by Parés and collaborators in the finite volume framework [8, 20] and which has later been extended to the discontinuous Galerkin finite element framework in [11, 22]. The Riemann solver used in this work is detailed in [16].

In the ADER-DG framework, the higher order in time is achieved with the use of an element-local space-time predictor, denoted by $\mathbf{q}_h(x,t)$ in the following, and which will be discussed in more detail later. Using (3.7), and after some computation on (3.8), we arrive to the following weak formulation,

$$\begin{aligned}
&\left(\int_{T_i} \Phi_k \Phi_l\, dx\right)\left(\hat{\boldsymbol{w}}_{i,l}^{n+1} - \hat{\boldsymbol{w}}_{i,l}^{n}\right) - \int_{t^n}^{t^{n+1}} \int_{T_i^\circ} \left(\partial_x \Phi_k \cdot \boldsymbol{F}_C(\mathbf{q}_h)\right) dxdt \\
&+ \int_{t^n}^{t^{n+1}} \Phi_{k,i+\frac{1}{2}} \mathcal{D}^-_{i+\frac{1}{2}}\left(\mathbf{q}^-_{h,i+\frac{1}{2}}, \mathbf{q}^+_{h,i+\frac{1}{2}}, {zb}^-_{h,i+\frac{1}{2}}, {zb}^+_{h,i+\frac{1}{2}}\right) + \Phi_{k,i-\frac{1}{2}} \mathcal{D}^+_{i-\frac{1}{2}}\left(\mathbf{q}^-_{h,i-\frac{1}{2}}, \mathbf{q}^+_{h,i-\frac{1}{2}}, {zb}^-_{h,i-\frac{1}{2}}, {zb}^+_{h,i-\frac{1}{2}}\right) dt \\
&\qquad + \int_{t^n}^{t^{n+1}} \int_{T_i^\circ} \Phi_k \left(\boldsymbol{P}(\mathbf{q}_h, \partial_x \mathbf{q}_h, \partial_x \eta_h) - \boldsymbol{T}(\mathbf{q}_h, \partial_x \mathbf{q}_h)\right) dxdt = \mathbf{0},
\end{aligned} \tag{3.9}$$

where T_i° corresponds to the interior of T_i and f_h stands for the projection of f onto the space $\mathcal{U}_h$. Moreover, $\mathcal{D}^\pm_{i\pm\frac{1}{2}}$ are the numerical flux at the cell interface given by the Riemann solver.

3.1. ADER-DG space-time predictor

We focus now on the computation of the predictor solution $\mathbf{q}_h(x,t)$, based on a weak formulation of the governing PDE system in space-time. The PDE system (2.1) is approximated with a so-called Cauchy problem *in the small*, i.e. without considering the interaction with the neighbour elements. Again, a similar space-time basis is considered to expand the predictor solution,

$$\mathbf{q}_h(x,t) = \sum_l \theta_l(x,t) \hat{\mathbf{q}}_l^i := \theta_l(x,t) \hat{\mathbf{q}}_l^i, \tag{3.10}$$

with the multi-index $l = (l_0, l_1)$ and where the space-time basis functions $\theta_l(x,t) = \varphi_{l_0}(\tau)\varphi_{l_1}(\xi)$ are again generated from the same one-dimensional nodal basis functions as before. Proceeding now similarly to the system (3.9), we multiply (3.1) by a space-time function and integrate over the space-time control volume $T_i \times [t^n, t^{n+1}]$. However, since we are only interested in an element local predictor solution, without interactions with the neighbor elements, the jump terms across interfaces are not taken into account. This leads to,

$$\begin{aligned}
&\int_{T_i} \theta_k(x,t^{n+1}) \mathbf{q}_h(x,t^{n+1})\, dx - \int_{T_i} \theta_k(x,t^n) \mathbf{q}_h^0(x,t^n)\, dx - \int_{t^n}^{t^{n+1}} \int_{T_i} \partial_t \theta_k(x,t) \mathbf{q}_h(x,t)\, dxdt \\
&\qquad = -\int_{t^n}^{t^{n+1}} \int_{T_i} \theta_k(x,t) \left(\partial_x \boldsymbol{F}_C(\mathbf{q}_h) + \boldsymbol{P}(\mathbf{q}_h, \partial_x \mathbf{q}_h, \partial_x \eta_h) - \boldsymbol{T}(\mathbf{q}_h, \partial_x \mathbf{q}_h)\right) dxdt.
\end{aligned} \tag{3.11}$$

Using the local space-time ansatz (3.10), Eq. (3.11) becomes a local nonlinear system for the unknown degrees of freedom $\hat{\mathbf{q}}_l^i$ of the space-time polynomials $\mathbf{q}_h$. The solution to the system can be found via a fixed point algorithm, that will converge, at most, in $N+1$ iterations for linear homogeneous systems. The initial guess $\mathbf{q}_h^0(x,t)$ for the iterative algorithm is simply set as the solution at time t^n, $\boldsymbol{w}_h(x,t^n)$.

This completes the description of the unlimited high order accurate and fully discrete ADER-DG schemes.

3.2. Preserving stationary solutions in the ADER-DG framework

We describe now the techniques developed to construct arbitrary high order ADER-DG numerical schemes that preserve exactly a set of stationary solutions corresponding to a stationary stratified fluid.

The first step consist on determining a local stationary solution $\boldsymbol{u}_{e,i}(x),\ x \in T_i$ of the family (2.5) at each time step. Although the stationary solution is calculated at each time step, we subsequentially drop the time dependence to simplify the notation. Notice that the family of stationary solutions (2.5) with $u_{\alpha,e,i} = 0,\ 1 \leq \alpha \leq M$ are fully determined by setting $h_{e,i}$ and $\theta_{1,e,i}, \dots \theta_{M,e,i}$. Particularly, $\bar{\eta}_i$,

$$\bar{\eta}_i = \frac{1}{\Delta x} \int_{x_{i-\frac{1}{2}}}^{x_{i+\frac{1}{2}}} \left(h_h(x,t^n) + z_{bh}(x)\right)\, dx,$$

where again we have denoted by f_h the discrete representation of f onto the polynomial space $\mathcal{U}_h$. Similarly, the constants $\theta_{1,e,i}, \dots \theta_{M,e,i}$ are computed solving,

$$\frac{1}{\Delta x} \int_{x_{i-\frac{1}{2}}}^{x_{i+\frac{1}{2}}} (h\theta)_{\alpha,e,i}(x, \bar{\eta}_i, \bar{\theta}_{\alpha,i}, \cdots, \bar{\theta}_{1,i})\, dx = \frac{1}{\Delta x} \int_{x_{i-\frac{1}{2}}}^{x_{i+\frac{1}{2}}} (h\theta)_{h,\alpha}(x,t^n)\, dx, \quad 1 \leq \alpha \leq M.$$

Using these constant, we are able to compute the stationary solution $\boldsymbol{u}_{e,i}(x)$. Note that this local stationary solutions satisfy the pressure terms (2.3) at each cell,

$$\boldsymbol{P}(\boldsymbol{u}_{e,i}, \partial_x \boldsymbol{u}_{e,i}, \partial_x \bar{\eta}_i) = 0. \tag{3.12}$$

Now, we could replace the numerical scheme (3.9) by the following well-balanced ADER-DG equivalent numerical scheme,

$$\begin{aligned}
&\left(\int_{T_i} \Phi_k \Phi_l\, dx\right)\left(\hat{\boldsymbol{w}}_{i,l}^{n+1} - \hat{\boldsymbol{w}}_{i,l}^{n}\right) - \int_{t^n}^{t^{n+1}} \int_{T_i^\circ} \left(\partial_x \Phi_k \cdot \boldsymbol{F}_C(\mathbf{q}_h)\right)\, dxdt \\
&+ \int_{t^n}^{t^{n+1}} \Phi_{k,i+\frac{1}{2}} \mathcal{D}_{i+\frac{1}{2}}^{-}\left(\mathbf{q}_{h,i+\frac{1}{2}}^{-}, \mathbf{q}_{h,i+\frac{1}{2}}^{+}, {z_b}_{h,i+\frac{1}{2}}^{-}, {z_b}_{h,i+\frac{1}{2}}^{+}\right) + \Phi_{k,i-\frac{1}{2}} \mathcal{D}_{i-\frac{1}{2}}^{+}\left(\mathbf{q}_{h,i-\frac{1}{2}}^{-}, \mathbf{q}_{h,i-\frac{1}{2}}^{+}, {z_b}_{h,i-\frac{1}{2}}^{-}, {z_b}_{h,i-\frac{1}{2}}^{+}\right)\, dt \\
&+ \int_{t^n}^{t^{n+1}} \int_{T_i^\circ} \Phi_k \left(\partial_x \boldsymbol{F}_C(\mathbf{q}_h) - \boldsymbol{T}(\mathbf{q}_h, \partial_x \mathbf{q}_h)\right)\, dxdt \\
&+ \int_{t^n}^{t^{n+1}} \int_{T_i^\circ} \Phi_k \left(\boldsymbol{P}(\mathbf{q}_h, \partial_x \mathbf{q}_h, \partial_x \eta_h) - \boldsymbol{P}((\boldsymbol{u}_{e,i})_h, \partial_x (\boldsymbol{u}_{e,i})_h, \partial_x (\eta_{e,i})_h)\right)\, dxdt = \mathbf{0},
\end{aligned} \tag{3.13}$$

Moreover, the extrapolated values at the intercells, denoted by $\mathbf{q}_{h,i\pm\frac{1}{2}}^{\pm}$, are computed in the following way,

$$\mathbf{q}_{h,i+\frac{1}{2}}^{-} = \boldsymbol{u}_{e,i}(x_{i+\frac{1}{2}}) + \hat{\boldsymbol{q}}_{h,i+\frac{1}{2}}^{-},$$

where $\hat{\boldsymbol{q}}_{h,i+\frac{1}{2}}^{-}$ is the extrapolation on the cell interface of the fluctuation $(\boldsymbol{q}_{h,i} - (\boldsymbol{u}_{e,i})_h)$, that is,

$$\hat{\boldsymbol{q}}_{h,i+\frac{1}{2}}^{-} = (\boldsymbol{q}_{h,i} - (\boldsymbol{u}_{e,i})_h)(x_{i+\frac{1}{2}}).$$

Similarly,

$$\mathbf{q}_{h,i+\frac{1}{2}}^{+} = \boldsymbol{u}_{e,i+1}(x_{i+\frac{1}{2}}) + \hat{\boldsymbol{q}}_{h,i+\frac{1}{2}}^{-},$$

where

$$\hat{\boldsymbol{q}}_{h,i+\frac{1}{2}}^{+} = (\boldsymbol{q}_{h,i+1} - (\boldsymbol{u}_{e,i+1})_h)(x_{i+\frac{1}{2}}).$$

A similar procedure is applied in the ADER step, where a high order local approximation of the solution $\boldsymbol{w}_h(x,t^{n+1})$ is computed by considering a fluctuation with respect to the local stationary solution $\boldsymbol{u}_{e,i}(x)$.

Finally, to clean possible spurious oscillations due to the absence of numerical viscosity in a stationary solution, we could perform the following procedure: first we compute the average of the fluctuation with respect to the local stationary solution,

$$\widehat{\boldsymbol{w}}_{h,i} = \frac{1}{\Delta x} \int_{x_{i-\frac{1}{2}}}^{x_{i+\frac{1}{2}}} \boldsymbol{w}_h(x,t^n) - \boldsymbol{u}_{e,i}(x)\, dx.$$

if $\left|\widehat{\boldsymbol{w}}_{h,i}\right|$ is less than a small threshold, then $\boldsymbol{w}_h(x,t^n)$ is redefined as follows,

$$\boldsymbol{w}_h(x,t^n) = \boldsymbol{u}_{e,i}(x) + \widehat{\boldsymbol{w}}_{h,i}.$$

4. Numerical test

We briefly demonstrate the capacity of the numerical scheme for preserving stationary solutions and to provide accurate results for complex density-driven flows. We first began considering a small perturbation of a lake-at-rest stationary solution with $M = 3$ and with the following non-constant bathymetry and free surface functions,

$$\eta(x,0) = 2 + \frac{1}{10}e^{-5\,x^2}, \qquad z_b(x) = \frac{1}{2}e^{-x^2},$$

defined in the channel with $x \in [-5,5]$ with just 50 elements and a forth order in space and time numerical scheme. Wall type boundary conditions are set and the initial condition for the relative density is given by equation (2.5) with the constant $\bar{\theta}_1 = 1.01$, $\bar{\theta}_2 = 0.02$ and $\bar{\theta}_3 = 0$. Figures 1 to 2 depicts the solution. As expected, a new stratified density profile is reached once a new free surface is achieved, and this new stationary solution is kept for long simulation times.

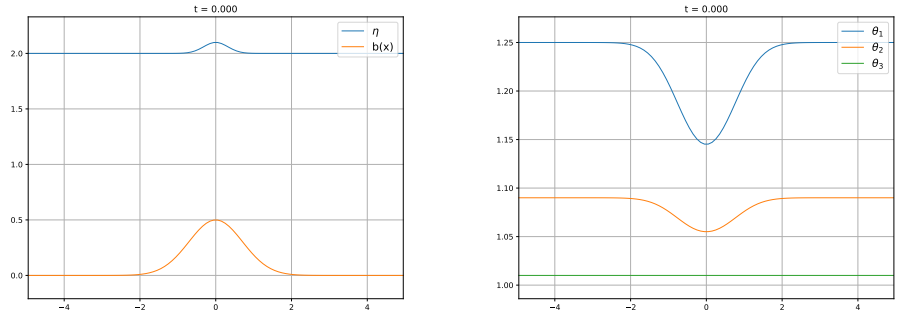

Fig. 1 Perturbation of a lake-at-rest steady state with non-constant density profile at $t = 0$ seconds. Left: free surface and bottom. Right: density profile.

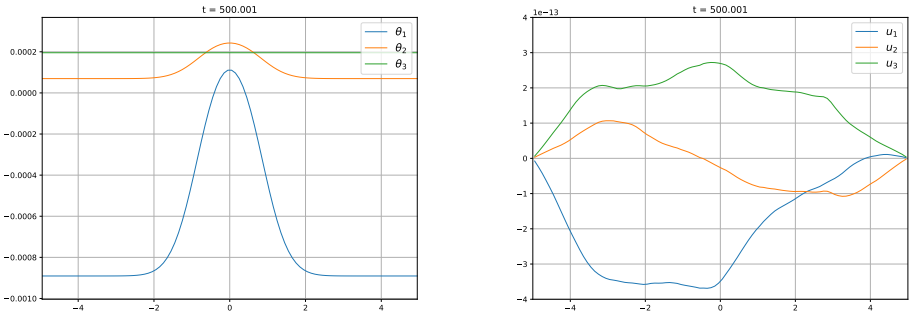

Fig. 2 Perturbation of a lake-at-rest steady state with non-constant density profile. Left: difference of relative densities between times $t = 500$ and $t = 0$ seconds. Right: velocity at time $t = 500$ seconds.

Finally, we show a simulation where a comparison with experimental laboratory data presented in [1]. We consider a flat channel $x \in [0,3]$ and a lock exchange of relative density between two fluids with density $\rho_0 = 1000\,\mathrm{Kg/m^3}$ and $\rho_1 = 1034\,\mathrm{Kg/m^3}$. The fluid with density ρ_1 is within a gatebox of 0.1 meters placed on the left of the channel, which is then released into the fluid ρ_1. The total height of the water is 0.3 meters. Figure 3 (left) depict the initial condition through a heat map of the relative density for a simulation with $M = 30$ layers and just 80 discretization points. To mimic the laboratory experiment in [1], wall-type boundary conditions are considered. Figure 3 (right) shows the simulation at final time $t = 25$ seconds, whereas figure 4 and 5 shows the evolution of the front position as the number of layers M increase. As we can see, we reach outstanding data agreement at approximately $M = 30$ layers.

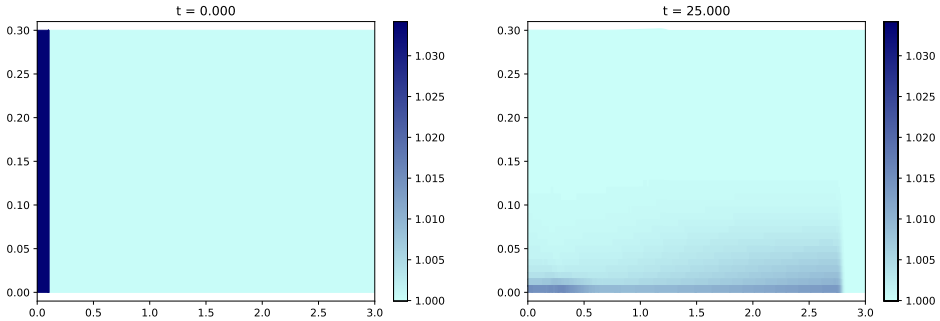

Fig. 3 Lock-exchange experiment in a flat channel: initial condition (left) and relative density at final time $t = 25$ seconds.

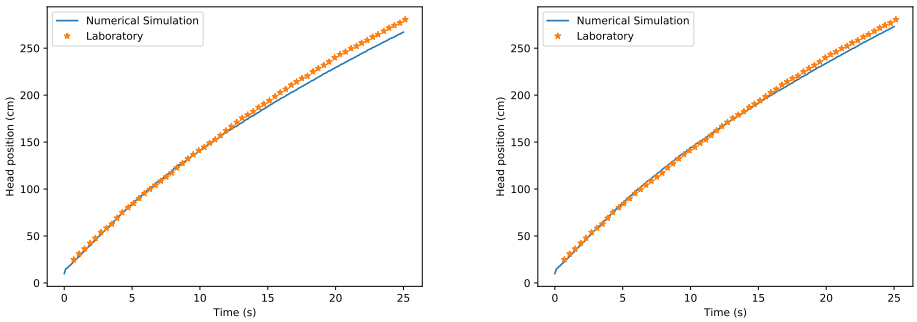

Fig. 4 Lock-exchange experiment in a flat channel: comparison on the evolution of the front position computed with the numerical scheme versus the laboratory data for 20 layers (left) and 25 layers (right).

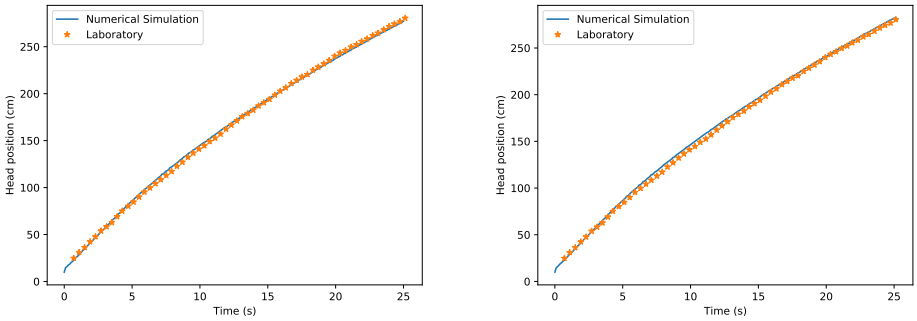

Fig. 5 Lock-exchange experiment in a flat channel: comparison on the evolution of the front position computed with the numerical scheme versus the laboratory data for 30 layers (left) and 40 layers (right).

5. Conclusions

We have briefly presented a novel discretization based on an ADER-DG numerical scheme for a shallow water model with a density dependent pressure term. The numerical scheme is arbitrary high order in space and time and exhibits great accuracy at smooth regions, while providing great results near strong discontinuities thanks to the MOOD strategy combined with a robust path-conservative solver. Finally, a novel strategy for preserving non-trivial stationary solutions in the ADER-DG framework has been presented. The numerical results are promising, showing excellent data agreement, and will help to increase our knowledge of density driven currents.

Acknowledgements

This research has been partially supported by the Spanish Government and FEDER through the coordinated Research project RTI2018-096064-B-C1 and RTI2018-096064-B-C2, The Junta de Andalucía research project P18-RT-3163 and the Junta de Andalucia-FEDER-University of Málaga Research project UMA18-FEDERJA-161.

References

[1] C. Adduce, G. Sciortino, and S. Proietti. Gravity currents produced by lock exchanges: Experiments and simulations with a two-layer shallow-water model with entrainment. *Journal of Hydraulic Engineering*, 138(2):111–121, 2012.

[2] E. Audusse, M.-O. Bristeau, M. Pelanti, and J. Sainte-Marie. Approximation of the hydrostatic navier–stokes system for density stratified flows by a multilayer model: Kinetic interpretation and numerical solution. *Journal of Computational Physics*, 230(9):3453 – 3478, 2011.

[3] Emmanuel Audusse and Marie-Odile Bristeau. A well-balanced positivity preserving "second-order" scheme for shallow water flows on unstructured meshes. *Journal of Computational Physics*, 206(1):311–333, 2005.

[4] Emmanuel Audusse and Marie-Odile Bristeau. Finite-volume solvers for a multilayer saint-venant system. *Applied Mathematics and Computer Science*, 17:311–320, 10 2007.

[5] Emmanuel Audusse, Marie-Odile Bristeau, Benoît Perthame, and Jacques Sainte-Marie. A multilayer saint-venant system with mass exchanges for shallow water flows. derivation and numerical validation. *ESAIM: Mathematical Modelling and Numerical Analysis*, 45(1):169–200, 2011.

[6] Alfredo Bermúdez and Ma Elena Vázquez. Upwind methods for hyperbolic conservation laws with source terms. *Computers & Fluids*, 23(8):1049–1071, 1994.

[7] François Bouchut and Vladimir Zeitlin. A robust well-balanced scheme for multi-layer shallow water equations. *Discrete and Continuous Dynamical Systems-series B*, 13:739–758, 06 2010.

[8] Manuel Castro, José M. Gallardo, and Carlos Parés. High order finite volume schemes based on reconstruction of states for solving hyperbolic systems with nonconservative products. applications to shallow-water systems. *Mathematics of Computation*, 75(255):1103–1134, 2006.

[9] Manuel J Castro and Carlos Parés. Well-balanced high-order finite volume methods for systems of balance laws. *Journal of Scientific Computing*, 82(2):48, 2020.

[10] M. de la Asunción, M.J. Castro, J.M. Mantas, and S. Ortega. Numerical simulation of tsunamis generated by landslides on multiple gpus. *Advances in Engineering Software*, 99:59 – 72, 2016.

[11] M. Dumbser, M. Castro, C. Parés, and E.F. Toro. ADER schemes on unstructured meshes for non-conservative hyperbolic systems: Applications to geophysical flows. *Computers and Fluids*, 38:1731–1748, 2009.

[12] Michael Dumbser and Claus-Dieter Munz. Building blocks for arbitrary high order discontinuous galerkin schemes. *Journal of Scientific Computing*, 27(1-3):215–230, 2006.

[13] Michael Dumbser, Olindo Zanotti, Raphaël Loubère, and Steven Diot. A posteriori subcell limiting of the discontinuous galerkin finite element method for hyperbolic conservation laws. *Journal of Computational Physics*, 278:47–75, Dec 2014.

[14] C. Escalante, M. Dumbser, and M.J. Castro. An efficient hyperbolic relaxation system for dispersive non-hydrostatic water waves and its solution with high order discontinuous galerkin schemes. *Journal of Computational Physics*, 394:385–416, 2019.

[15] Enrique Fernández-Nieto, E H. Koné, and T Chacón Rebollo. A multilayer method for the hydrostatic navier-stokes equations: A particular weak solution. *Journal of Scientific Computing*, 60, 08 2014.

[16] Ernesto Guerrero Fernández, Manuel Jesús Castro-Díaz, and Tomás Morales de Luna. A second-order well-balanced finite volume scheme for the multilayer shallow water model with variable density. *Mathematics*, 8(5):848, 2020.

[17] Nouh Izem, Mohammed Seaid, and Mohamed Wakrim. A discontinuous galerkin method for two-layer shallow water equations. *Mathematics and Computers in Simulation*, 120:12–23, feb 2016.

[18] Miguel Lastra, José M Mantas, Carlos Ureña, Manuel J Castro, and José A García-Rodríguez. Simulation of shallow-water systems using graphics processing units. *Mathematics and Computers in Simulation*, 80(3):598–618, 2009.

[19] Jorge Macias, Manuel J. Castro, José Manuel González-Vida, Marc de la Asunción, and Sergio Ortega. HySEA: An operational GPU-based model for Tsunami Early Warning Systems. In *EGU General Assembly Conference Abstracts*, EGU General Assembly Conference Abstracts, page 14217, May 2014.

[20] C. Parés. Numerical methods for nonconservative hyperbolic systems: a theoretical framework. *SIAM Journal on Numerical Analysis*, 44(1):300–321, 2006.

[21] William H Reed and TR Hill. Triangular mesh methods for the neutron transport equation. Technical report, Los Alamos Scientific Lab., N. Mex.(USA), 1973.

[22] S. Rhebergen, O. Bokhove, and J.J.W. van der Vegt. Discontinuous Galerkin finite element methods for hyperbolic nonconservative partial differential equations. *Journal of Computational Physics*, 227:1887–1922, 2008.